NUMERICAL INVESTIGATION OF TURBULENT NATURAL CONVECTION IN REACTOR PRESSURE VESSEL LOWER PLENUM DURING CORE MELTDOWN SCENARIO

Andrej Horvat, Ivo Kljenak
Reactor Engineering Division
"Jožef Stefan" Institute
Ljubljana, Slovenia
E-mail: andrej.horvat@ijs.si

ABSTRACT - A possible severe accident scenario is a general meltdown and relocation of the reactor core during which molten core material accumulates in the lower plenum of the reactor vessel. The decay heat generated in a radioactive material would have to be removed through the walls of the lower plenum in order to ensure the integrity of the reactor pressure vessel. Numerical simulations of turbulent natural convection in a geometry representing the lower plenum cavity of a reactor pressure vessel were conducted. A two-dimensional numerical code based on a finite-volume method was developed to simulate turbulent natural convection in a fluid with internal heat generation using large-eddy simulation. Simulations were performed at Rayleigh numbers 10^{10} and $2 \cdot 10^{11}$ and Prandtl numbers 1.2, 7 and 8, which corresponds to conditions in the numerical investigations made by Nourgaliev et al. (1997) and in the experimental work done by Asfia and Dhir (1996). The results are shown to be in satisfactory agreement.

NOMENCLATURE

b	modified pressure
G	filter operator
h, T	temperature
I	heat generation
l	filter width
L	length scale
Nu	Nusselt number $(qL_0)/(\alpha\,(T_w - T_{aver}))$
Pr	Prandtl number ν_0/υ_0
q	heat flux
Ra	Rayleigh number $(\lvert\vec{g}\rvert\beta_0 I_0 L_0^5)/(\nu_0\lambda_0\upsilon_0)$
$\underline{S}$	tensor of subgrid stresses
$\underline{T}$	strain tensor
v	velocity
x, z	spatial coordinates

Greek Letters

β	thermal dilatation
ν	kinematic viscosity
λ	thermal conductivity
ζ	specific heat
ρ	density
υ	thermal diffusivity

Subscripts / Superscripts

0	scale value
res	residuum $(h - \overline{h})$
tr	trace of tensor
w	value at the wall

INTRODUCTION

Natural convection heat transfer in liquid pools with internal heat generation has been the subject of a considerable number of fundamental and applied research programmes. This process determines the thermal and fluid dynamic behaviour of many natural systems and industrial instalations, such as the earth's mantle, welding pools, electrically heated melt pools in metallurgy and material processing, etc.

Recently, natural convection heat transfer in internally heated liquid pools has been related to molten core behaviour during severe accidents in nuclear reactors. A possible severe accident scenario is a general meltdown and relocation of the reactor core during which molten core material accumulates in the lower plenum of the reactor vessel. External cooling of the lower plenum by flooding of the concrete cavity with subcooled water is one of the management strategies currently being considered for this type of accident. Our purpose was to study natural convection behaviour in the lower plenum during this specific scenario. In the past, a considerable amount of experimental and analytical effort was used to obtain heat transfer correlations for natural convection of internally heated fluids in various geometries, such as in a fluid layer, in rectangular, semi-circular and elliptical "slice-type" cavities and in hemispherical pools. A review of experimental and theoretical results is presented in the work of Nourgaliev et al. (1997).

Among recent analytical efforts to predict these phenomena, two major approaches can be distinguished. The first approach can be recognized, for instance, in the works of Henry and Fauske (1992), Henry and Suh (1994), and Suh and Henry (1993), who developed integral models using discrete volumes. The second approach has been used, among others, by Dinh and Nourgaliev (1997), Dinh et al. (1997), and Nourgaliev et al. (1997), who used a differential model of transport equations. The first approach provides only integral values of thermal-hydraulic variables but requires less computer time. The second approach, which was also selected in the present work, provides a more detailed picture of the physical phenomena but requires extensive computer capacities due to modeling of the fluid turbulence.

The fluid behaviour in the considered process depends on two dimensionless parameters, namely the Prandtl (*Pr*) and Rayleigh (*Ra*) numbers. When the Rayleigh number exceeds a certain value, transition from laminar to turbulent flow occurs. There are very little published simulation results at Rayleigh numbers beyond $Ra=10^{10}$. Because of the scale of fluid motion, which is smaller than the numerical grid spacing, a proper model of turbulence is necessary to ensure the consistency of numerical results.

In the past, attempts to model turbulence in fluids with internal heat generation were made by using various k-ε models. In this work, a modified Smagorinsky-type of large-eddy simulation (LES) was used. This model proved to be a robust and reliable numerical tool for solving turbulent natural convection cases in a fluid with internal heat generation.

GEOMETRICAL CONSIDERATIONS, BOUNDARY AND INITIAL CONDITIONS

Although some experimental and numerical results for semi-circular and ellyptical cavities are already available, a square cavity was assumed to simplify calculations at high Rayleigh numbers. Fig. 1 shows a schematic of the lower plenum arrangement and boundary conditions during a core meltdown scenario, whereas fig. 2 shows the supposed qualitative behaviour of a fluid with internal heat generation in a rectangular geometry, based on the calculated results.

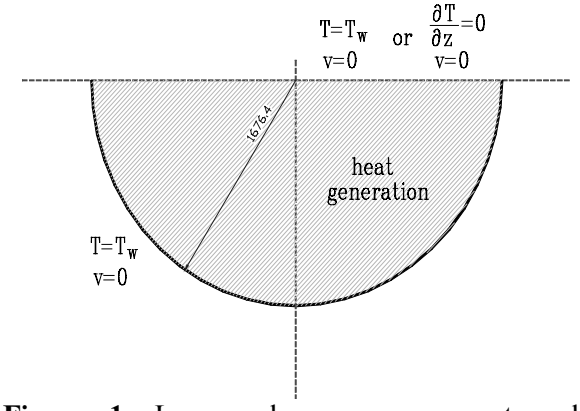

Figure 1. Lower plenum arrangement and boundary conditions during a core meltdown scenario.

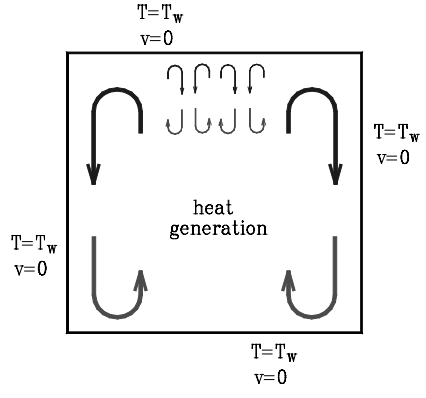

Figure 2. Schematic of qualitative behaviour of fluid with internal heat generation in a rectangular geometry.

The comparison of experimental results from natural convection cases in rectangular and spherical cavities reveals the similarity of heat transfer processes in both geometries. Moreover, it is safe to assume that the maximum heat transfer, based on Nusselt number, is similar for rectangular and spherical cavities of similar dimensions. The maximum heat transfer occurs in the upper corners of the cavities. Larger discrepancies between heat transfer in rectangular and spherical cavities occur only in the lower parts (Asfia and Dhir, 1996; Nourgaliev et al., 1997).

Experimental and numerical results presented by Dinh et al. (1997) and Nourgaliev et al. (1997) suggest that the fluid pattern is basically two-dimensional. A two-dimensional model should thus be adequate for simulation of the considered phenomenon.

In the present calculations, the wall was considered isothermal because of melting and solidification processes which occur in the lower plenum during meltdown scenario. No-slip boundary conditions were prescribed for velocities. A homogeneous isothermal temperature field was applied for the initial stage of simulations.

PHYSICAL MODEL

The above presented phenomenon may be described with the continuity, momentum and energy equations for an incompressible fluid with variable density using the so-called Boussinesq's approximations :

$$\nabla \cdot \vec{v} = 0 \quad , \tag{1}$$

$$\frac{\partial \vec{v}}{\partial t} + \nabla \cdot \left(\vec{v} \otimes \vec{v}\right) = -\nabla b + \mathrm{Pr}\left(\nabla \cdot \underline{T}\right) - \mathrm{Ra}\,\mathrm{Pr}\, h \frac{\vec{g}}{|\vec{g}|} \quad , \tag{2}$$

$$\frac{\partial h}{\partial t} + \nabla \cdot \left(h \vec{v}\right) = -\nabla \vec{q} + I \quad . \tag{3}$$

In the derivation of eq. (2), it was assumed that density differences result only from temperature variations. Composition variations were thus neglected. When equations are discretized, they have to be filtered in order to remove the unresolved motion. In this work, a spatial "top-hat" filter was used, which is also widely used in large-eddy type of turbulence models (Eidson, 1985; Germano, 1991).

$$G(R-r) = \begin{cases} 1/2\Delta r, & |R-r| \le \Delta r \\ 0, & |R-r| > \Delta r \end{cases} \quad , \quad \overline{h}(t,r) = \int_{-\infty}^{\infty} G(R-r)\, h(t,r)\, dr \quad , \tag{4}$$

where r is any of the space coordinates. Although the choice of filter width is in principle arbitrary, it seems plausible to prescribe it as proportional to the size of the numerical grid. Application of the filter operation (4) to equations (1)-(3) leads to:

$$\nabla \cdot \overline{\vec{v}} = 0 \quad , \tag{5}$$

$$\frac{\partial \overline{\vec{v}}}{\partial t} + \nabla \cdot \left(\overline{\vec{v}} \otimes \overline{\vec{v}}\right) = \nabla \overline{b} + \mathrm{Pr}\left(\nabla \cdot \underline{\overline{T}}\right) - \mathrm{Ra}\,\mathrm{Pr}\, \overline{h} \frac{\vec{g}}{|\vec{g}|} - \nabla \cdot \left({}^{res}\underline{S}\right) \quad , \tag{6}$$

$$\frac{\partial \overline{h}}{\partial t} + \nabla \cdot \left(\overline{h}\, \overline{\vec{v}}\right) = -\nabla \cdot \overline{\vec{q}} + I - \nabla \cdot \left({}^{res}\vec{q}\right) , \tag{7}$$

where the last terms of eqs. (6) and (7) represent the unresolved part of the velocity and temperature fields:

$${}^{res}\underline{S} = \overline{\left(\vec{v} \otimes \vec{v}\right)} - \left(\overline{\vec{v}} \otimes \overline{\vec{v}}\right) \quad , \tag{8}$$

$${}^{res}\vec{q} = \overline{\left(h\vec{v}\right)} - \left(\overline{h}\, \overline{\vec{v}}\right) \quad . \tag{9}$$

Using Boussinesq's approximation of turbulent stresses and turbulent thermal fluxes (Hinze,1959), these terms are added to the strain tensor in eq. (6) and to the energy diffusion fluxes in eq. (7).

We write:

$$ {}^{res}\underline{S} = -\nu_f \underline{\overline{T}} + \frac{1}{2}\delta_{j,i}\, {}^{res}\underline{S}_{tr} \quad , \tag{10} $$

$$ {}^{res}\vec{q} = \upsilon_f \vec{q} \quad , \tag{11} $$

and further:

$$ \frac{\partial \overline{\vec{v}}}{\partial t} + \nabla \cdot \left(\overline{\vec{v}} \otimes \overline{\vec{v}} \right) = -\nabla \overline{b} + \left(\mathrm{Pr} + \nu_f \right) \left(\nabla \cdot \underline{\overline{T}} \right) - \mathrm{Ra}\,\mathrm{Pr}\,\overline{h}\,\frac{\vec{g}}{|\vec{g}|} \quad , \tag{12} $$

$$ \frac{\partial \overline{h}}{\partial t} + \nabla \cdot \left(\overline{h}\,\overline{\vec{v}} \right) = -\left(1 + \frac{\nu_f}{\mathrm{Pr}_f} \right) \nabla \cdot \overline{\vec{q}} + I \quad . \tag{13} $$

The eddy viscosity was modeled with the Kolmogorov assumption (Hinze ,1959):

$$ \nu_f = const.\, l_f^{4/3} \varepsilon^{1/3} \, . \tag{14} $$

It was further assumed that the filter splits the spectra of subgrid motion somewhere in the Kolmogorov equilibrium region and that the turbulence viscous dissipation is equal to the turbulence production. The turbulence production can be easily defined from filtered values. Thus:

$$ \nu_f = const.\, l_f^2 \; S \sqrt{1 - Ri} \tag{15} $$

where

$$ S = \frac{1}{2} \left(\underline{T} : \underline{T} \right) \quad , \tag{16} $$

$$ Ri = \left(\frac{\mathrm{Pr}\,\mathrm{Ra}}{\mathrm{Pr}_f} \frac{\vec{q}}{S} \right) \cdot \frac{\vec{g}}{|\vec{g}|} \quad . \tag{17} $$

The constant in eqs. (14) and (15) is case-dependent and determined empirically. In our case its value was prescribed as $(0.21)^2$, whereas the turbulent Prandtl's number Pr_f was set equal to 0.4, as reported by Eidson (1985).

As the above described turbulent model is too dissipative in the vicinity of the wall (Eidson, 1985), wall functions had to be used. In our case, we selected van Driest's function (Patankar and Spalding, 1970), which was modified to account for buoyancy forces:

$$ f_\mu = 1 - \exp(-x/26 \;\; f(Ri)) \quad , \tag{18} $$

$$ \text{where } f(Ri) = \begin{cases} 1 + \tanh(-\pi\, Ri) & , Ri > 0 \\ 1 + \log(-\pi\, Ri + 1), & Ri < 0 \end{cases} \quad . \tag{19} $$

NUMERICAL METHOD

A finite-volume numerical method was used to solve the set of equations (5), (12) and (13) with no-slip boundary conditions for the velocity field and Dirichlet's type of boundary conditions for the temperature field. A 128x128 points staggered grid was used for spatial discretisation. The convection term in the equation of motion (12) was discretised using a second-order accurate Harlow and Welch scheme (1965), whereas the energy equation convection term was discretised using a second-order up-wind scheme. This was necessary to ensure stability of integration.

The time integration of the equations was performed using an explicit second-order accurate Adam-Bashford method. The method was slightly modified to account for time step variations during integration. Calculations, which were performed on a Sun Ultra 2 workstation, required from 24 to 120 hours of CPU time till steady-state conditions were reached.

RESULTS AND DISCUSSION

Numerical simulations were performed at Rayleigh numbers $Ra = 10^{10}$ and $2 \cdot 10^{11}$ and Prandtl numbers Pr = 1.2, 7, and 8. A picture of general circulation pattern of a fluid with internal heat generation was already shown on fig. 2. An example of calculated instantaneous velocity field is presented on fig. 3. It can be seen that the fluid rises in the core of the cavity as it is driven by buoyancy forces. It is then cooled at the upper plate and forms an unstable boundary layer which is able to make an intrusion of cold fluid in the upper core region. The small vorticals may clearly be observed on fig. 4.

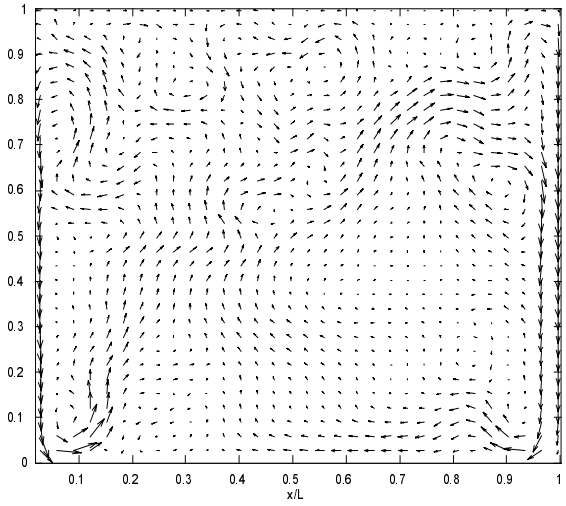

Figure 3.
Circulation of a fluid with internal heat generation.

These intrusions are probably the major contributors to turbulence production. The boundary layer of cold fluid is stabilized at the side wall where the fluid descends to the bottom of the cavity. If the friction of the rising fluid at the core side of the boundary layer is strong enough, part of the descending stream will separate from the rest and change direction before reaching the bottom.

The lower part of the core of the cavity is stratified with increasing temperature from bottom to top. It was observed during calculations that the stability of temperature stratification increases with increasing Pr number.

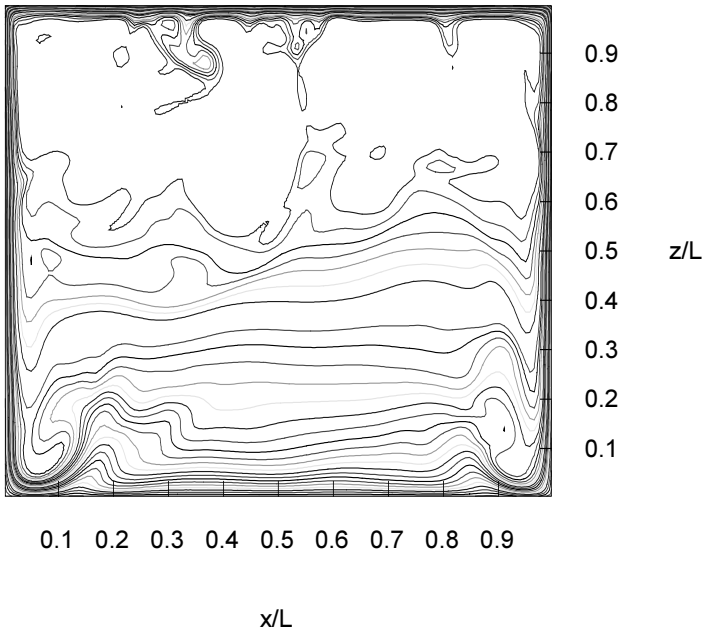

Figure 4.
Example of temperature field at $Ra = 10^{10}$ and Pr = 1.2.

Figure 5 provides an insight into the turbulent behaviour of the above described system. The vertical coordinate represents the subgrid kinetic energy, defined as :

$$k = \left({}^{res}\vec{v}\,,\ {}^{res}\vec{v} \right) / \left(\bar{\vec{v}}, \bar{\vec{v}} \right) . \tag{20}$$

As shown on fig. 5, the turbulence is not evenly distributed over the cavity. Rather the strong local extremes occur. The unresolved part of the kinetic energy represents in some regions even 20% of the resolved kinetic energy of the fluid. This shows that turbulence in fluid with internal heat generation should not be neglected in lower plenum modeling.

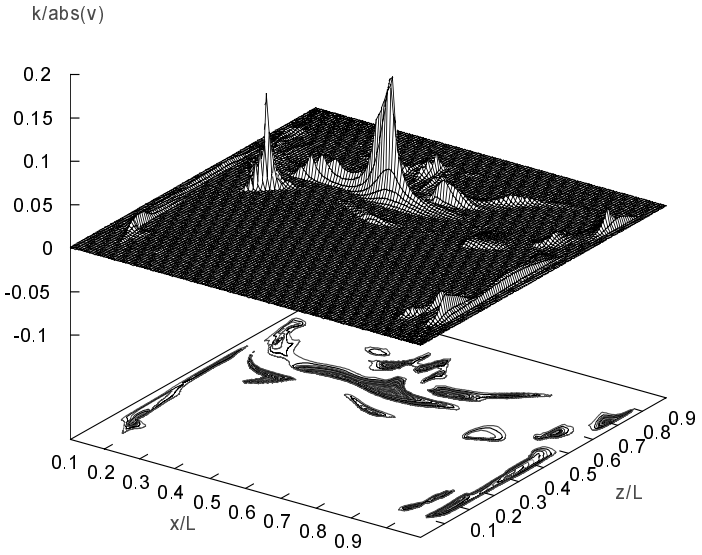

Figure 5.
Subgrid kinetic energy at $Ra = 10^{10}$ and $Pr = 1.2$

The variable of interest from the engineering point of view is the wall heat transfer. Local and average *Nu* numbers were calculated for bottom, side and top walls for three different *Pr* numbers and two different *Ra* numbers. The obtained results are summarized and compared to calculations performed by Nourgaliev et al. (1997) for a square cavity at $Ra = 10^{10}$ and to experimental results obtained by Asfia and Dhir (1996) in a spherical pool at $Ra = 2 \cdot 10^{11}$ in table 1. The agreement between results is satisfactory.

Table 1: *Nu* number averaged over bottom and top wall

	Bottom wall	**Top wall**
Nourgaliev et al. (1997) /our predictions, $Ra = 10^{10}, Pr = 1.2$	13.9/14.3	67.6/73.1
Nourgaliev et al. (1997) /our predictions, $Ra = 10^{10}, Pr = 7$	10.1/10.5	76.2/81.2
Asfia and Dhir (1996) /our predictions, $Ra = 2 \cdot 10^{11}, Pr = 8$	(-) /15.6	164.6/168.3

It was found that at given *Ra* number the *Nu* number assumes the highest values in the upper corners of the cavity (figs.6 and 7). The variation of *Pr* number strongly affects the flow conditions on side walls and at the bottom. It was observed during simulations that increasing of *Pr* number causes tearing of the boundary layer and turbulence production. This may be seen on the distribution of *Nu* number along the side walls (figs. 8 and 9).

At the bottom of the cavity the variation of *Pr* number has the strongest influence. At smaller *Pr* number, the influence of viscous dissipation is weaker. The vorticals are more resistant and the stratification of the lower part of the core region is less stable, which can be seen on figs.10 and 11. This also influences the local *Nu* number which exhibits peaks at a certain distance from the bottom corners.

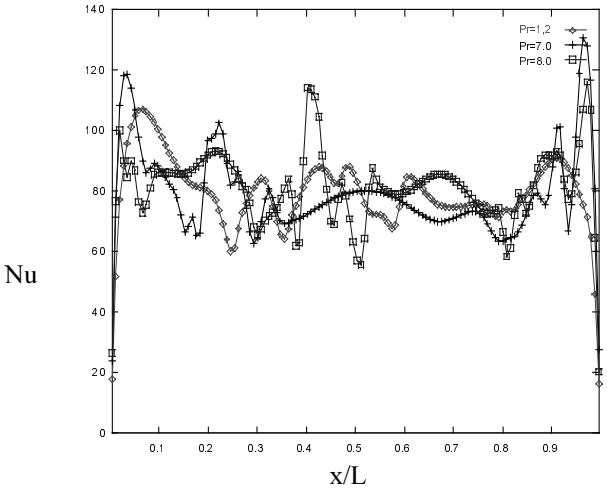

Figure 6. *Nu* number at the cavity top wall $Ra = 10^{10}$ and Pr =1.2, Pr =7.0, Pr =8.0.

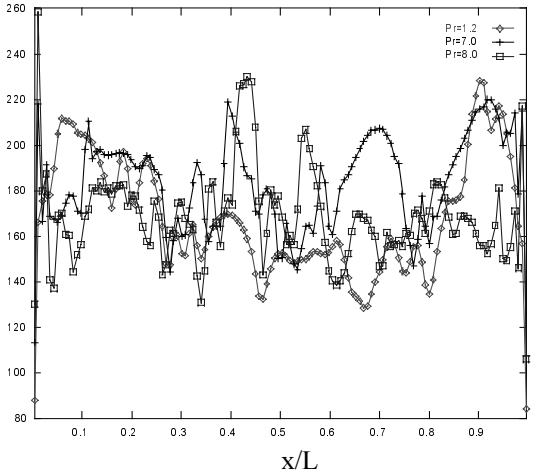

Figure 7. *Nu* number at the cavity top wall $Ra = 2 \cdot 10^{11}$ and Pr =1.2, Pr =7.0, Pr =8.0.

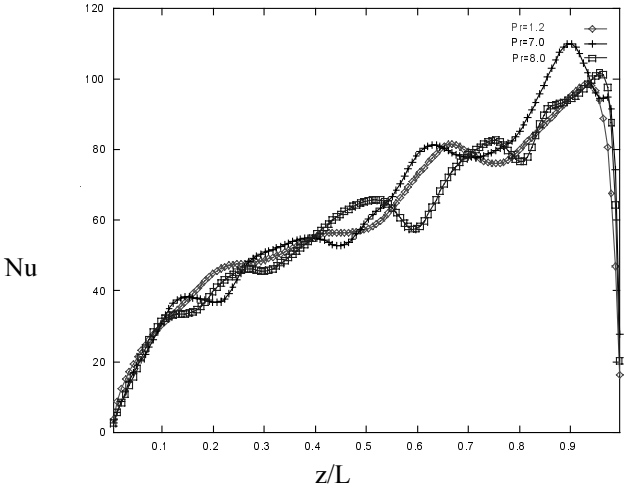

Figure 8. *Nu* number at the cavity side wall $Ra = 10^{1}$ and Pr =1.2, Pr =7.0, Pr =8.0.

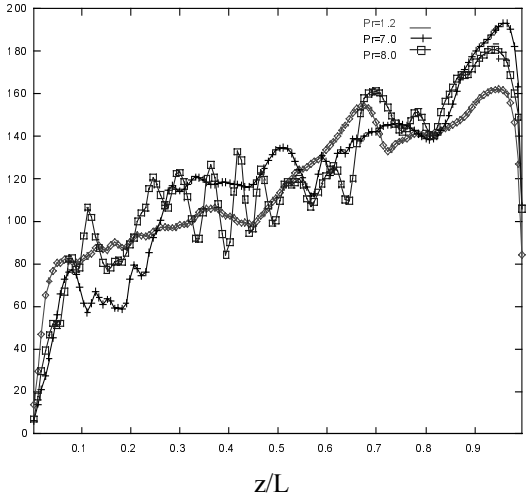

Figure 9. *Nu* number at the cavity side wall $Ra = 2 \cdot 10^{11}$ and Pr =1.2, Pr =7.0, Pr =8.0.

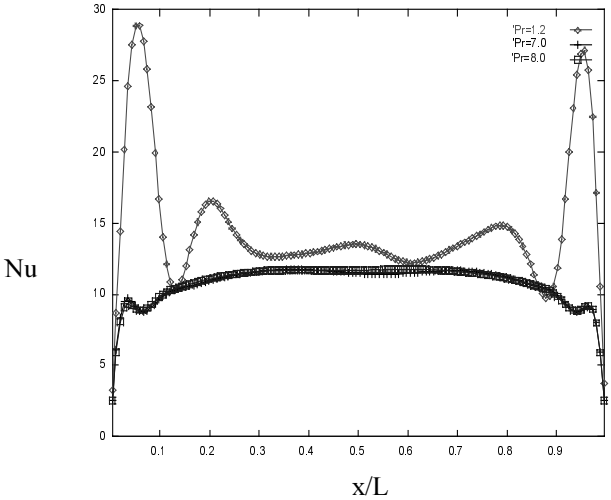

Figure 10. *Nu* number at the cavity bottom wall $Ra = 10^{10}$ and Pr =1.2, Pr =7.0, Pr =8.0.

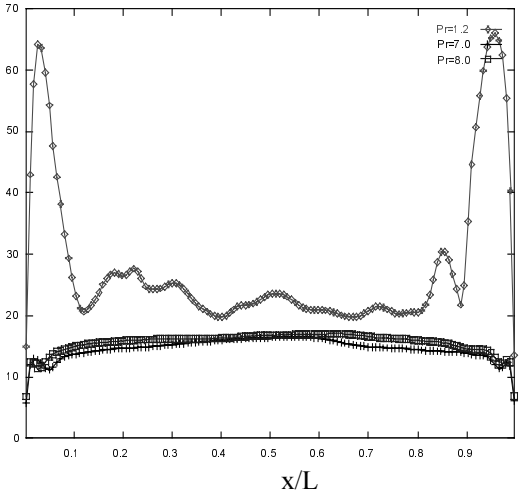

Figure 11. *Nu* number at the cavity bottom wall $Ra = 2 \cdot 10^{11}$ and Pr =1.2, Pr =7.0, Pr =8.0.

CONCLUSIONS

A modified Smagorinsky-type large eddy simulation of natural convection in a fluid with internal heat generation was developed. The process was simulated in a square cavity which represents the lower plenum of a reactor pressure vessel filled with molten core material.

Results, which were obtained for Rayleigh numbers 10^{10} and $2 \cdot 10^{11}$ and Prandtl numbers 1.2, 7 and 8, show good agreement with theoretical results from Nourgaliev et al. (1997) and experimental results from Asfia and Dhir (1996). The proposed approach thus seems to be appropriate for modeling of lower plenum cooling problems.

It was observed that a lower *Pr* number, stratified layers in the cavity lower region are disturbed by descending flows in the convection-dominated side wall region and by falling cold fluid from the top wall region. The local *Nu* number in the bottom corners of the cavity is also significantly increased.

Further improvements of the proposed model will be directed towards modeling of natural convection in a spherical geometry in order to reduce uncertainties due to geometrical simplifications.

REFERENCES

Asfia, F.J., Dhir, V.K., 1996, "An Experimental Study of Natural Convection in a Volumetrically Heated Spherical Pool Bounded on Top with a Rigid Wall", Nucl.Eng.Design, Vol. 163, pp. 333-348.

Dinh, T.N., Nourgaliev, R.R., 1997, "Turbulence Modelling for Large Volumetrically Heated Liquid Pools", Nucl.Eng.Design, Vol. 169 , pp. 131-150.

Dinh, T.N., Nourgaliev, R.R., Sengal, B.R., 1997, "On Heat Transfer Characteristics of Real and Simulant Melt Pool Experiment", Nucl.Eng.Design, Vol. 169 , pp. 151-164.

Eidson, T. M., 1985, "Numerical Simulation of the Turbulent Rayleigh-Bernard Problem Using Subgrid Modeling", J.Fluid Mech., Vol. 158, pp. 245-268.

Germano, M., 1992, "Turbulence: The Filtering Approach", J. Fluid Mech., Vol. 238, pp. 325-336.

Harlow, F.H., Welch, J.E., 1965, "Numerical Calculation of Time-Dependent Viscous Incompressible Flow of Fluid with Free Surface", Phys.Fluids, Vol. 8, No. 12, pp. 2182-2186.

Henry, R.E., and Fauske, H.K., 1992, "External Cooling of a Reactor Vessel under Severe Accident Conditions", Nucl.Eng.Design, Vol. 139, pp. 31-43.

Henry, R.E., and Suh, K.Y., 1994, "Integral Analysis of Debris Material and Heat Transport in Reactor Vessel Lower Plenum", Nucl.Eng.Design, Vol. 151, pp. 203-221.

Hinze, J. O., 1959, "Turbulence", McGraw-Hill, 2nd ed., p. 23.

Nourgaliev, R.R., Dinh, T.N., Sengal, B. R., 1997, "Effect of Fluid Prandtl Number on Heat Transfer Characteristics in Internally Heated Liquid Pools with Rayleigh Numbers up to $10^{12"}$, Nucl.Eng. Design, Vol. 169 , pp. 165-184.

Patankar, S. V., Spalding, D. B., 1970, "Heat and Mass Transfer in Boundary Layers", Intertext Books, London, p. 21.

Suh, K.Y., Henry R.E., 1993, "Integrated Modeling of Debris Bed Heat and Mass Transfer in the PWR Lower Plenum for Severe Accident Analysis", ANS 1993 Winter Meeting, San Francisco, California, USA, Nov. 14-18, Ninth Proceedings of Nuclear Thermal Hydraulics, pp. 38-49.